Journal of Medicinal Chemistry

Article

pubs.acs.org/jmc

Dabigatran and Dabigatran Ethyl Ester: Potent Inhibitors of Ribosyldihydronicotinamide Dehydrogenase (NQO2)

Simon Michaelis,[‡] Anett Marais, Anna K. Schrey, Olivia Y. Graebner, Cornelia Schaudt, Michael Sefkow, Friedrich Kroll, Mathias Dreger, Mirko Glinski,[†] Hubert Koester, Rainer Metternich,[†] and Jenny J. Fischer*[,‡]

caprotec bioanalytics GmbH, Volmerstrasse 5, 12489 Berlin, Germany

Supporting Information

ABSTRACT: Recent studies have revealed that compounds believed to be highly selective frequently address multiple target proteins. We investigated the protein interaction profile of the widely prescribed thrombin inhibitor dabigatran (**1**), resulting in the identification and subsequent characterization of an additional target enzyme. Our findings are based on an unbiased functional proteomics approach called capture compound mass spectrometry (CCMS) and were confirmed by independent biological assays. **1** was shown to specifically bind ribosyldihydronicotinamide dehydrogenase (NQO2), a detoxification oxidoreductase. Molecular dockings predicted and biological experiments confirmed that dabigatran ethyl ester (**2**) inhibits NQO2 even more effectively than the parent **1** itself. Our data show that **1** and **2** are inhibitors of NQO2, thereby revealing a possible new aspect in the mode of action of **1**. We present a workflow employing chemical proteomics, molecular modeling, and functional assays by which a compound's protein-interaction profile can be determined and used to tune the binding affinity.

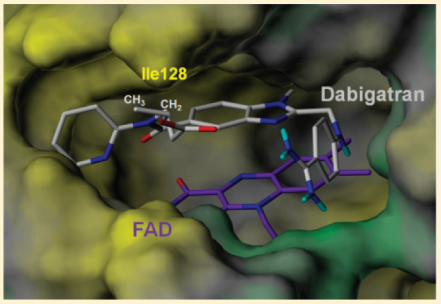

INTRODUCTION

In drug discovery, the dominant paradigm is that maximally selective ligands should be designed to act on single drug targets.[1] In the last years, it has however become evident that many effective drugs act via modulation of multiple proteins rather than on individual targets.[1−3] For some drugs, e.g., the atypical antipsychotics, a promiscuous pharmacological profile is the key point for their efficacy.[4] Cheminformatics have played a crucial role in prediction of new targets for given drugs or therapeutic areas.[4−9] However, not all protein structures and mechanisms guiding small-molecule protein interactions are known and therefore these theoretical computational approaches currently require experimental data to formulate or test their hypothesis. Thus, unbiased experimental methods are needed to complete the target space. Compiling experimental protein interaction profiles of small-molecule drugs gives novel insights into their mode of action, thereby generating a better understanding of the structure−activity relationship (SAR), toxicology, and repurposing possibilities. Repurposing of established safe drugs has become a major focus of interest, as new drug candidates dramatically fail during clinical trials due to toxicity or insufficient efficacy.[10] Such profiling investigations have been carried out mainly for promiscuous drugs such as kinase inhibitors[11,12] but also for small molecules targeting histone deacetylases.[13,14] Anticoagulants such as dabigatran[15] (**1**, Figure 1) are believed to have very clear-cut targets such as inhibition of factor II (thrombin) of the blood coagulation cascade.[15]

We here investigate for the first time the protein interaction profile of an anticoagulant and chose **1**, which has been described as a particularly safe drug.[16] Its prodrug dabigatran etexilate is currently in clinical trials for long-term use for the prevention of stroke and non-CNS systemic embolism. Despite its drug safety, not all off-targets and potential novel targets of **1** have been identified. An unbiased method to compile small-molecule−protein interaction profiles is capture compound

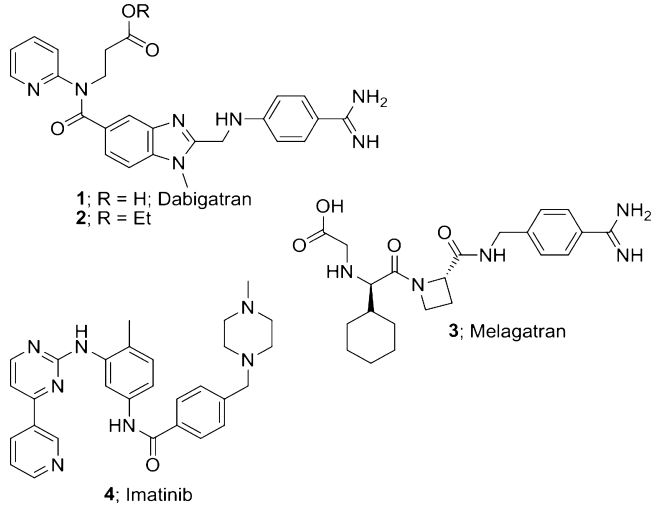

Figure 1. Structures of thrombin inhibitors **1**−**3** and tyrosine kinase inhibitor **4**.

Received: January 30, 2012
Published: April 11, 2012

ACS Publications © 2012 American Chemical Society

dx.doi.org/10.1021/jm3001339 | J. Med. Chem. 2012, 55, 3934−3944

mass spectrometry (CCMS, Scheme 1), which employs small-molecule based probes called capture compounds (CCs) containing the compound of interest as selectivity function. We report the synthesis of CCs and a subsequent chemical proteomics investigation which revealed that **1** specifically binds and functionally inhibits ribosyldihydronicotinamide dehydrogenase (NQO2), a phase II detoxification oxidoreductase, with similar inhibitory potential as the known NQO2 inhibitor imatinib (**4**, Figure 1).[17] On the basis of molecular modeling, we then hypothesized and could indeed show experimentally that dabigatran ethyl ester (**2**, Figure 1) has higher affinity than **1** to both thrombin and NQO2. We present a strategy how to determine the protein targets of a small-molecule compound in an unbiased way in a native biological environment and how such data can be employed to modify interaction properties of the drug molecule.

Scheme 1. Schematic CCMS Workflow[a]

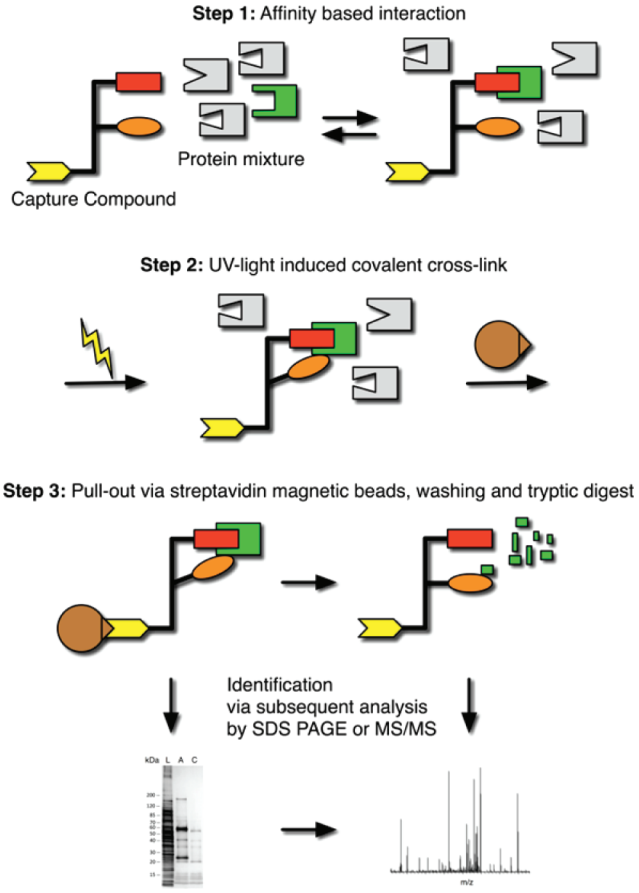

[a]CCs are trifunctional molecules: the selectivity function (red) binds target proteins (green) through reversible affinity interaction, a covalent bond between the photo-reactivity function (orange) and the protein(s) is generated. The crosslinked proteins are isolated via the biotin sorting function (yellow) using streptavidin magnetic beads and identified by MS or visualized by using standard gel protocols. As controls, additional competition experiments using the respective drugs were carried out.

RESULTS AND DISCUSSION

To investigate the protein interaction profile of **1** for the identification of novel specific binders, we rely on CCMS experiments (Scheme 1) with both CCs derived from **1** and CCs of melagatran (**3**, Figure 1), a closely related peptide mimetic thrombin inhibitor to compare the interaction profiles. As chemical modifications of a parent drug may facilitate interactions with different target proteins,[18] we chose two attachment positions to the CCs' scaffold (Scheme 2, **X**) for each drug (Supporting Information Figure S1). This resulted in two CCs **5** and **6** derived from **1** and two CCs **7** and **8** derived from **3** (Scheme 2A). The aim was to obtain a picture of the compound−protein interaction profiles that should be as complete as possible, i.e., identification of interactions occurring at the acid and at the amidine side of the compounds.

The synthesis route to CC **5**−**8** is depicted in Scheme 2. Briefly, commercially available dabigatran ethyl ester acetate was equipped with an aliphatic linker to give compound **11**. Removal of the Boc protecting group followed by coupling to the CC scaffold[19] and saponification yielded CC **6** (Scheme 2B). CC **8** was available from Boc-protected amino acid **13**. Subsequent coupling of **13** with an aliphatic linker, Boc deprotection, and coupling to the peptidic building block gave **15**. Intermediate **15** was converted into **8** by subsequent Boc deprotection, coupling with methyl 2-(4-nitrophenylsulfonyloxy)acetate, removal of the nitrobenzenesulfonamide protecting group, coupling to the scaffold, and saponification (Scheme 2C). CCs **5** and **7** were prepared in one step from **1** and **3**, respectively. All CCs **5**−**8** were thermally and biologically stable, and only the expected photoreaction products were formed upon UV-irradiation.

Next, we carried out capture assays with purified recombinant human thrombin to elucidate whether the thrombin binding properties are retained in the CCs. As predicted by crystal structures,[20,21] both CCs **5** and **7** bearing a terminal amidine group, specifically bound thrombin while CCs **6** and **8** with opposite attachment orientations showed no or little interaction with thrombin (Figure 2). According to the known binding mode of **1** into the thrombin binding pocket, the benzamidine group forms tight interactions with Asp189 located in the bottom of the primary specificity pocket. This pocket should not fit any modifications on the amidine group of the inhibitor because it is very narrow. The ratio between the signals in the lanes was 0.8:0.3:1:0 for CCs **5**:**6**:**7**:**8** as determined by densitometric analysis. We believe the unexpected detection with CC **6** is due to unspecific background cross-linking caused by the artificial situation in which a single purified protein is used as compared to a complex lysate samples. As expected, no signals were observed in the gel lanes with CC **6** and **8**.

We started our investigations of the protein interaction profile of **1** in parallel to **3** by performing CCMS experiments (Scheme 1) in the hepatocyte derived cell line HepG2. Enrichment and isolation of specifically interacting proteins was carried out using CCs **5**−**8** in four independent replicate experiments. The captured and trypsinized proteins were identified using a high resolution LTQ Orbitrap hybrid mass spectrometer. Only proteins identified with more than 99% probability and at least two unique peptides with 95% probability were considered to be identified with sufficient confidence. In competition control experiments, an excess of the respective free drugs was added that compete with the corresponding CC for specific binding sites. Therefore, proteins that are detected by LC-MS in the capture assay and that are significantly diminished in competition control experiments are defined to be specific. The specificity is quantified by the fold change between assay and competition (Figure 3). Moreover,

dx.doi.org/10.1021/jm3001339 | J. Med. Chem. 2012, 55, 3934−3944

Scheme 2. (A) Structures of CCs 5 and 6, CCs 7 and 8, and CCs 9 and 10; (B) Synthesis of CC 6; (C) Synthesis of CC 8[a]

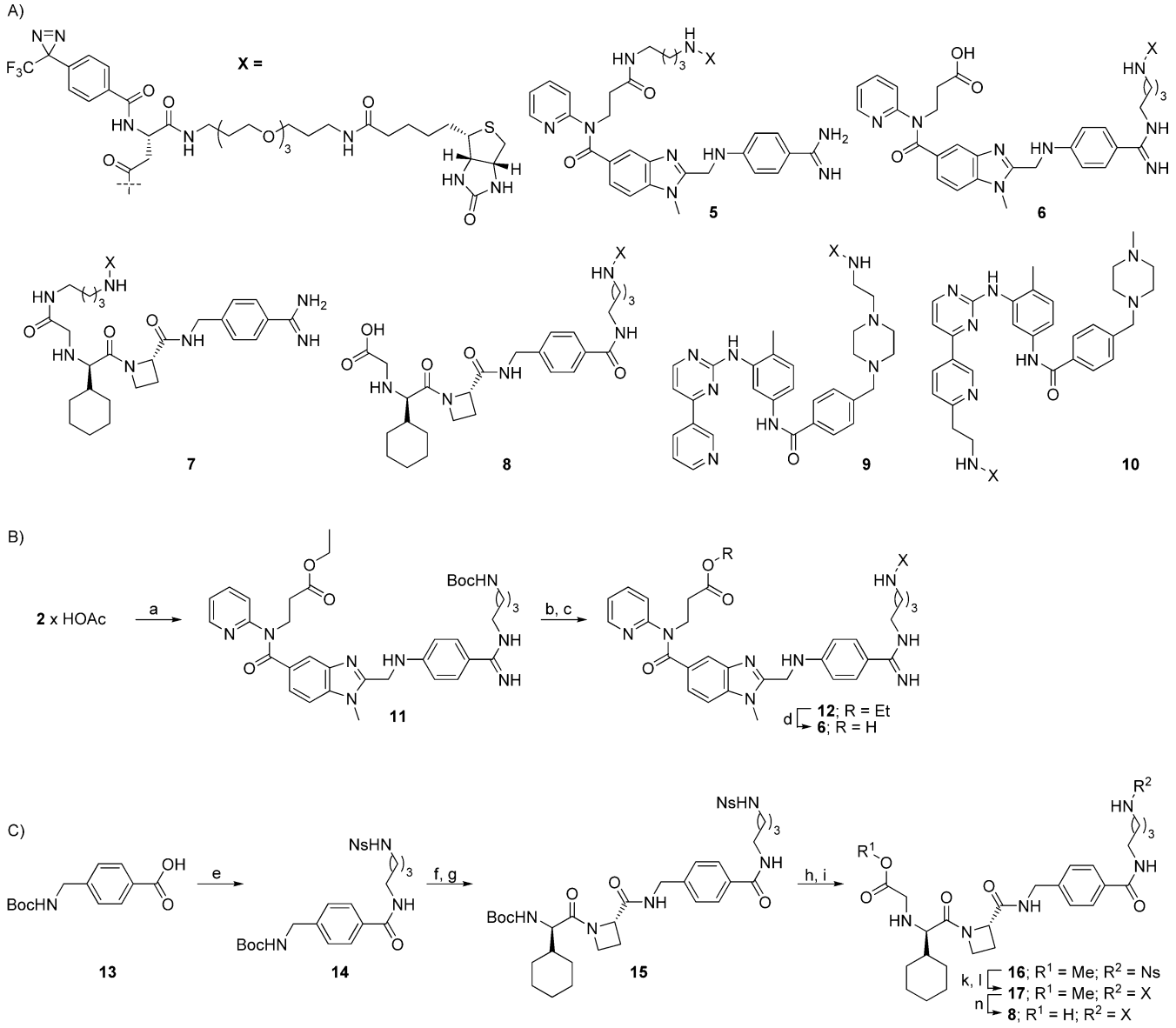

[a]Conditions: (a) *tert*-butyl 4-aminobutylcarbamate, EtOH, 78 °C, 12 h, 91%; (b) TFA, DCM, 0 °C, 1 h, used as crude; (c) X−OH, HATU, DIPEA, DMA, 23 °C, 2 d, 35% over two steps; (d) LiOH, THF/water, 4 °C, 17 h, 48%. Conditions for (C): (e) *N*-(4-aminobutyl)-4-nitrobenzenesulfonamide, HATU, DIPEA, DMAP, DMA, 23 °C, 1.5 h, 85%; (f) TFA, DCM/MeOH, 40 °C, 2 h, used as crude; (g) (*S*)-1-((*R*)-2-(Boc-amino)-2-cyclohexylacetyl)azetidine-2-carboxylic acid, HATU, DIPEA, DMA, 23 °C, 2 d, 96% over two steps; (h) TFA, DCM, 0 °C, 0.5 h, used as crude; (i) methyl 2-(4-nitrophenylsulfonyloxy)acetate, K_2CO_3, MeCN, 60 °C, 1.5 h, non-pure product used as such; (k) 2-mercaptoacetic acid, DBU, MeCN, 0 °C, 1 h, used as crude; (l) X−OH, HATU, DIPEA, DMA, 23 °C, 17 h, 43% over two steps; (n) LiOH, THF/water, 0 °C, 1 h, 78%.

experiments were carried out in quadruplicate, allowing the determination of significance (*p*-value from Student's *t* test). Only proteins fulfilling stringent enrichment criteria of high specificity (fold change ≥2) and at the same time high significance (*p*-value ≤0.05, corresponding to a $-\log_{10}$ (*p*-value ≥1.3) were considered as specific binders of the respective drug (these specific binders are indicated in the boxed area, Figure 3 and also listed in Table 1).

Seven proteins fulfilled these criteria for at least one of the investigated CCs: NQO2, HYOU1, HNMT, HNRPC, and ADK specifically bound CCs **5** or **6** and VPS35 and LRC59 showed specific interaction with CC **8**, but CC **7** showed no significantly enriched proteins. An overview of the significantly enriched proteins is given in Table 1. In a previous study,[13] we analyzed a quantity of tryptically digested HepG2 input cell lysate, comparable to the protein amounts obtained in the CCMS experiments presented here. Out of the seven proteins enriched here, only HYOU1 and HNRPC were among the 360 proteins identified from HepG2 input lysate. This shows that NQO2, HNMT, ADK, VPS35, and LRC59 are in too low abundance for the detection limit of the used LC-MS method without prior specific enrichment by CCMS. NQO2 belongs to proteins not expressed at sufficient level to be identified by LC-MS from HepG2 whole cell lysate, at least when using our standard setting. However, NQO2 can be identified robustly and specifically after enrichment by CCMS. This shows that

dx.doi.org/10.1021/jm3001339 | *J. Med. Chem.* 2012, 55, 3934−3944

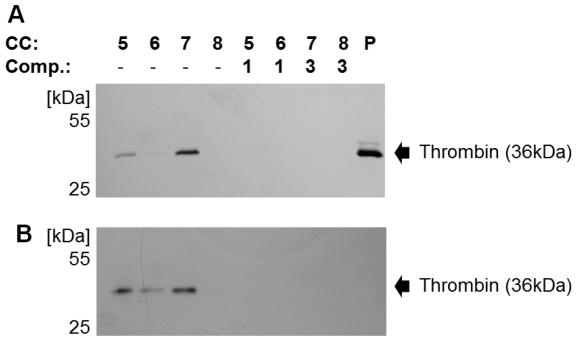

Figure 2. Purified human recombinant thrombin is captured by CCs **5** and **7** but not by **6** and **8**. (A) Silver stained SDS-PAGE shows specific enrichment. (B) Anti-biotin blot of the same experimental setup demonstrates covalent cross-linking of CCs **5** and **7** to thrombin. Competition controls (Comp.) were preincubated with **1** or **3** as indicated. P = 0.3 μg thrombin protein input control.

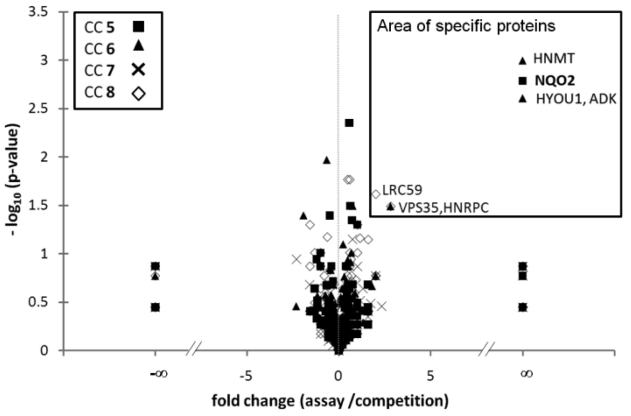

Figure 3. Volcano plot of quadruplicate CCMS experiments using CCs **5**–**8** in HepG2 lysate. Specific proteins (boxed area) are reproducibly identified in capture assays but not in competition controls and therefore exhibit high fold change (x-axis) and significant p-value (y-axis).

CCMS can identify even proteins expressed at low level because of the enrichment procedure. In the case of CCMS, the covalent bond formed between the target protein and the CC allows for stringent washing steps during the isolation process, and this facilitates enrichment even of weak binders and low abundant proteins.[22]

Robust and specific identification of NQO2 as interactor of **1** caught our particular interest: the oxidoreductase NQO2 has been suggested[11] to be the direct target in resveratrol induced inhibition of cancer cell growth[23−25] and to play an important role in metabolism of xenobiotics.[26] Therefore, different inhibitors for NQO2 have been developed and investigated in recent years.[27]

We decided to confirm the enrichment of NQO2 by CC **5** in a second cell line. Since the leukemia cell line K562 has been used in several previous studies investigating NQO2, we chose K562 for our investigations.[11,17,28] In one of these studies, Bantscheff et al.[11] identified NQO2 as the first nonkinase off-target of **4** through pull down experiments with immobilized **4**. Consequently, we chose **4** and its CCs **9** and **10** (Scheme 2A) as positive controls for the following experiments. We repeated the capture experiments followed by LC-MS based protein identification with CCs **5**–**8** in parallel with CCs **9** and **10** in independent duplicate experiments in K562 cell lysate (Supporting Information Table S2). We confirmed NQO2 as specific target of **1** and **4** by specific enrichment of NQO2 through CCs **5** and **9** followed by mass spectrometry identification. In addition, we carried out Western Blots using an NQO2 specific antibody to confirm the identification of NQO2 as specifically enriched protein by an independent detection method in both cell types (Figure 4A and Supporting Information Figure S4A). Specific interaction of **1** with NQO2 was also confirmed by Western Blot in microsomes derived from a pool of human liver donor samples (Supporting Information Figure S4B).

To show direct binding of **1**, we then carried out capture experiments with pure recombinant NQO2 (Figure 4B). Cross-competition experiments using a CCs **5** and **6** and competing with **4** or vice versa (Figure 4C) demonstrated that the inhibitors **1** and **4** target the same binding pocket.

Orientation specificity of CCs **5** and **6** and cross-competition with **4** gave first experimental insights into the binding mode of **1** to NQO2. On the basis of our data and published NQO2 crystal structures, we computed a molecular model. The active form of NQO2 is dimeric and comprises two active sites (Supporting Information Figure S5). The quinone binding pocket is formed by FAD bound to one chain and residues

Table 1. Proteins Significantly Enriched by CCMS Experiments using CCs 5−8 in HepG2 Cell Lysate[a]

protein	SwissProt ID	full name	function	M_w [kDa]	PI[b]	compound[c]	fold change[d]	p-value[e]	enriched in K652 lysate[f]
NQO2	P16083	ribosyldihydronicotinamide dehydrogenase	dehydrogenase	26	5.88	**5**	∞	0.0016	yes
HNMT	P50135	histamine *N*-methyltransferase	methyltransferase	33	5.18	**6**	∞	0.0099	no
HYOU1	Q9Y4L1	hypoxia up-regulated protein 1	hypoxia up-regulated protein 1	111	5.07	**6**	∞	0.0024	no
HNRPC	P07910	heterogeneous nuclear ribonucleoproteins C1/C2	function in mRNA processing and splicing	34	4.95	**6**	∞	0.0025	no
ADK	P55263	adenosine kinase	kinase	41	6.25	**6**	2.8	0.0321	no
LRC59	Q96AG4	leucine-rich repeat-containing protein 59	membrane protein of the ER with unknown function	35	9.61	**8**	2	0.0240	no
VP35	Q96QK1	vacuolar protein sorting-associated protein 35	essential component of the retromer complex	92	5.32	**8**	2.8	0.0321	no

[a]All protein properties were retrieved from SwissProt Database if not indicated otherwise. [b]Calculated isoelectric point. [c]CC with which the named protein was enriched from HepG2 cell lysate. [d]Ratio of the spectral counts with which the protein was identified in the four capture assays and in the four competition controls (A/C). In cases where the number of spectral counts in the competition was zero, this value is ∞. [e]Significance of enrichment in the four capture assays compared to the four competition controls as determined by Student's t test. [f]The capture experiments in K652 cells were carried out in duplicate as additional controls.

dx.doi.org/10.1021/jm3001339 | J. Med. Chem. 2012, 55, 3934−3944

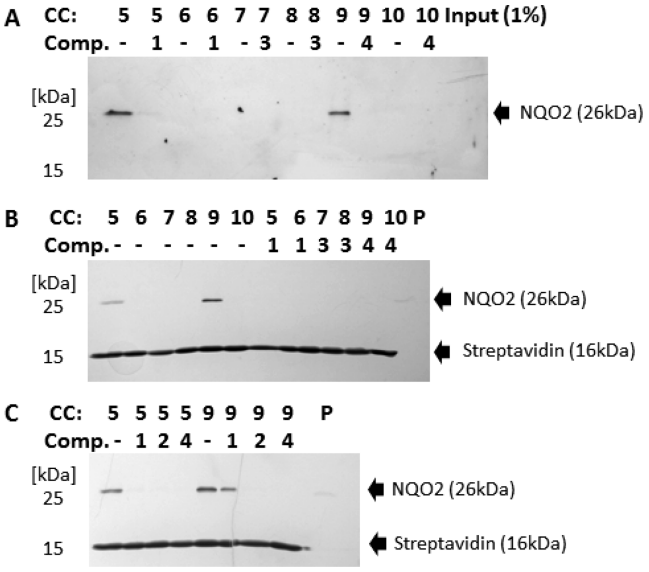

Figure 4. NQO2 is specifically captured and enriched by CC **5** and CC **9**. (A) Enrichment of endogenous NQO2 from HepG2 lysate detected by anti-NQO2 Western Blot. (B) Silver stained SDS-PAGE showing direct interaction of **1** with NQO2 by capturing of human purified recombinant NQO2 protein. (C) **1**, **2**, and **4** occupy the same NQO2 binding site, as demonstrated by cross-competition experiments visualized by silver stained SDS-PAGE. Final concentrations of CCs 5 μM and competitors 100 μM, P = 0.3 μg of recombinant NQO2.

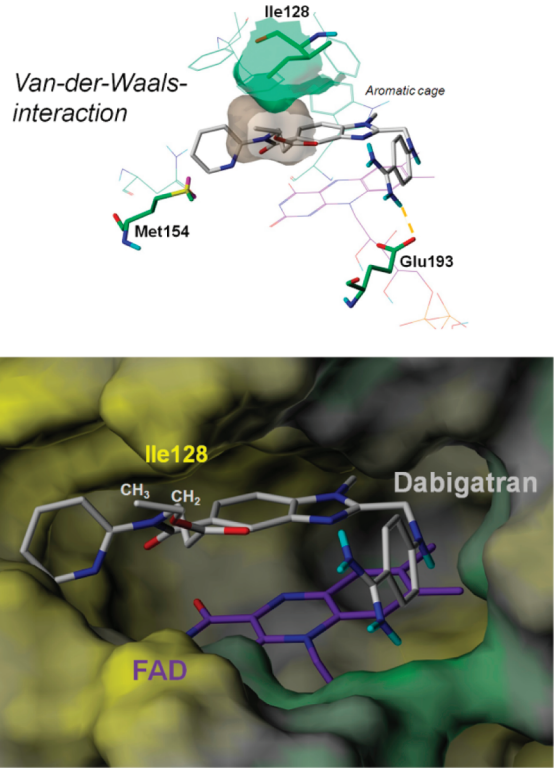

Figure 5. Molecular model showing **2** (gray) bound to NQO2. Protein residues are depicted in green, the cofactor FAD in purple. (top) Crucial binding residues: Glu193 exhibits a salt bridge to the amidine groups of **1** and **2**. An aromatic cage consisting of several Phe and Tyr residues interacts with the central aromatic core. Met154 and Ile128 interact via Van der Waals interactions. The interaction of Ile128 with the ethyl group of **2** (Van der Waals radii of these moieties are shown as translucent surfaces) should stabilize binding of **2** rather than **1** in accordance with the experimental data. (bottom) Surface of the binding pocket colored by lipophilic potential (green, hydrophilic; yellow, lipophilic).

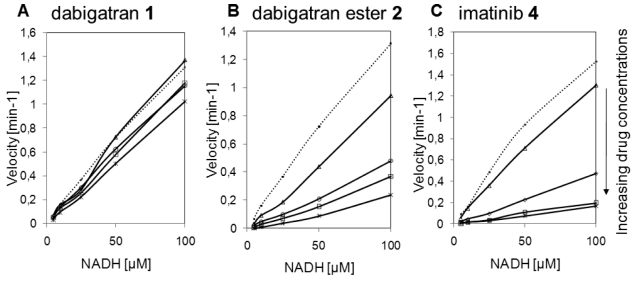

Figure 6. Michaelis Menten plots showing functional inhibition of NQO2 catalysis by **1** (A) and by **2** (B). **4** (C) was used as positive control. Experiments were carried out twice acquiring duplicate data points per experiment.

from both chains and can harbor a flat, aromatic ligand lying coplanar to the flavones redox center, stabilized by π-interactions. This is the case for the central core of **1**, but not of **3**, thus explaining selective binding of **1** over **3**. The amidine of **1** is part of a hydrogen-bond network, whereas the acid functionality protrudes into the solvent, explaining the orientation specificity. Our model also clarifies why the closest relative of NQO2, which is NQO1 with 49% sequence identity, was not specifically isolated: NQO1s Phe233 and Phe237 make the catalytic pocket too narrow for **1**. Because the acid functionality of **1** is surrounded by hydrophobic residues, we speculated that the more lipophilic ester **2** would further stabilize the interaction between NQO2 and **1** (Figure 5) (additional models as well as sequence alignment of NQO2 and NQO1 are given in the Supporting Information).

We decided to experimentally follow up the modification suggested by our model and investigated competition of CC **5** binding to recombinant NQO2 using **1** and **2** as competitors (Supporting Information Figure S8). The concentrations at which half of the NQO2 signal was lost were 10 μM for **1** and 1.5 μM for its ester **2**, demonstrating almost 1 order of magnitude stronger interaction of the ester over acid **1**.

We then investigated the functional inhibition of NADH-dependent mitomycin C metabolism[17] by NQO2 using **1** and **2** as inhibitors as well as **4** as positive control (Figure 6). The K_i values were computed using Sigma Plot 10. IC_{50} values were calculated based on Michaelis Menten kinetics for competitive inhibition. **1** competitively and concentration-dependently inhibited activated NQO2. The K_i could be approximated to 70 μM and the IC_{50} to 60 μM. Notably, **2** exhibits a much higher inhibitory potential on NQO2 in the assay described, with a K_i = 0.9 μM and an IC_{50} = 0.8 μM. The half maximal inhibitory concentration of **4** was 0.34 μM in accordance with the literature (Supporting Information Figure S10).[17] A summary of all affinity and inhibition data generated is given in Table 2.

1 is administered in the form of an ester to increase the bioavailability,[15] therefore both forms (the ester and the drug) are present. We determined the K_i of 2 toward NQO2 to be 0.9 μM and the IC_{50} to be 0.8 μM, thus we expect a contribution to the mode of action. Because we could show functional inhibition of recombinant NQO2 by **1** and **2** and also binding of **1** and **2** to endogenous NQO2 within whole cell lysates and lysates derived from human liver microsomes (Figure 4A and

dx.doi.org/10.1021/jm3001339 | J. Med. Chem. 2012, 55, 3934−3944

Table 2. Affinities and Functional Inhibition between 1, 2, and 4 and NQO2 or Thrombin

	CC		
assay	1	2	4
half maximal competition of NQO2 binding through CC 5 (μM)[a]	11	1.5	nd
IC_{50}, functional inhibition of NQO2 (μM)[b]	>10	0.8	0.40
K_i, functional inhibition of NQO2 (μM)[c]	60	0.9	nd
IC_{50}, functional inhibition of thrombin (nM)[d]	13.8	1.2	nd

[a]Details are given in the Supporting Information, Figures S8 and S9. [b]Details are given in Supporting Information, Figure S10. [c]Details are given in Figure 6. [d]Details are given in Supporting Information, Figure S11.

Supporting Information Figure S4), these compounds should also be active within the cellular context of the cytosol where NQO2 is located. Although it is to be expected that the ester will be hydrolyzed, the more active precursor **2** will in part contribute to the mode of action of dabigatran. The extent of this contribution will depend strongly on its pharmacokinetics, protein binding, and on the patients (e.g., with decreased liver function) treated with the drug molecule.

To investigate whether the modification of **1** also affected its inhibitory potential toward thrombin, we analyzed the proteolytic properties of thrombin in the presence of **1** and **2**, respectively. For **1**, we determined an IC_{50} value of 14 nM toward thrombin, which is in good accordance with the value of 10 nM reported previously.[20,29] In the case of **2**, the inhibitory potential was even increased by 1 order of magnitude (1.2 nM, Supporting Information Figure S11). NQO2 is a flavoprotein that catalyzes the 2-electron reduction of various quinones, redox dyes, and the vitamin K menadione. NQO2 predominantly uses dihydronicotinamide riboside (NRH) as the electron donor. The possible physiological relevance of NQO2 inhibition by **1** or **2** remains to be tested. In fact, the finding that **2** is 1 order of magnitude more active on thrombin than **1** is quite surprising considering the X-ray studies of **1** the thrombin system published by Hauel et al.[20] Here, the carboxylate group protrudes into bulk solvent, exhibiting no interactions with the protein. However, a more hydrophobic moiety like an ethyl ester could adopt a conformation that would allow hydrophobic contacts of the whole chain to the rim of the pocket.

One single heavy atom can increase the overall binding energy by max 1.5 kcal/mol, which correlates to approximately 1 order of magnitude in the binding constant, although the average binding per atom decreases with increasing heavy atom count.[30,31] We calculated the ligand binding efficiencies (LE: atom-count dependent binding description)[30] and the fit qualities (FQ: normalized LEs)[31] for both **1** and **2**. For both compounds, we calculated FQ values of around 0.6 for thrombin and FQ values of around 0.4 for NQO2.

Bigger ligands in general[30,31] and **1** in particular[20] are known to interact mainly by hydrophobic interactions. Thus the ratio of the interacting surfaces of **1** and its ethyl ester should be in the range of the ratio of the p*K* values. We calculated a ratio of 0.88−0.91, which is in good correlation with the p*K* ratio from the NQO2 binding assay (0.86). Supporting Information Figure S12 shows that the ethyl ester group of **2** significantly extends the interaction surface especially with hydrophobic amino acids such as Ile 128 and Met 154 (for details of the LE calculations and interaction surfaces see Supporting Information).

Taken together, our experimental and modeling results clearly show the direction in which to modify the structure of **1** in order to tune its binding properties toward higher affinity. This was indeed reflected by the inhibitory effect on enzyme functions in vitro. While at present the physiological effects of these interactions remain open, the strategy devised here indicates that capture compound mass spectrometry-driven drug profiling not only reveals the interaction profile of the drug molecule but also can generate critical data that can guide medicinal chemistry efforts to redesign a drug molecule toward new properties.

CONCLUSION

In summary, we here identified NQO2 as novel target for the thrombin inhibitor **1** by using a workflow combining medicinal chemistry, proteomics, and molecular modeling. Our study is in line with the notion that small-molecule drugs specifically interact not only with one target protein but with a set of target proteins. At least one of the previously unknown interactions we identified for **1** is functionally relevant in vitro. Furthermore, we were able to show that the ethyl ester of **1** has improved the binding properties toward both NQO2 and thrombin, resulting in higher affinity. In the context of NQO2 inhibition by resveratrol,[32] prevention of toxic effects by metabolism of xenobiotics as well as reduction of cancer cell growth through NQO2 inhibitors have been described.[32−35] Our findings suggest that it might be interesting to further investigate the possible effect of the interaction between **1** and NQO2 on the overall mode of action of **1**. The results also show for the first time how CCMS can be employed, not only to identify a drug's interactors and elucidate its mechanism of action but also how these results can be used to tune the binding properties of a given drug in the desired direction.

EXPERIMENTAL SECTION

Chemistry. Unless otherwise noted, all reactions were performed in dry glassware and under argon. Commercially available reagents and solvents were used as received without further purification. Column chromatography was carried out by using Geduran Si 60 silica gel from Merck. MPLC purification was performed on a Buechi system (Buechi control unit C-620; 2 Buechi pump modules C-605; column, omnifit (230 × 15 mm); stationary phase, LiChroprep RP-select B 25−40 μm; Buechi UV photometer C-635; Buechi fraction collector C-660; mobile phase A, 0.1% AcOH Millipore grade; mobile phase B, MeCN prepsolv grade). LCT was carried out on a Waters system (HPLC pump Waters 1525; autosampler CTC HTS PAL; column oven Techlab K7 (40 °C); diode array detector Waters 2998 (200−600 nm); MS detector Waters LCT mass spectrometer equipped with an electrospray ion source). LCT method A: column, Phenomenex Mercury MS (20 mm × 2 mm); stationary phase, Phenomenex Synergi Fusion RP, 2.5 μm; guard column Phenomenex Security Guard, Synergi Fusion RP; flow 0.4 mL/min; mobile phase A, 0.1% HCOOH Millipore grade; mobile phase B, MeCN LC-MS grade; 10% B to 40% B in 9 min; 40% B to 100% B in 2 min; 100% B for 4 min. LCT method B: column, Phenomenex Kinetex (50 mm × 3 mm); stationary phase, Phenomenex Kinetex C18, 2.6 μm, 100 Å; guard column Phenomenex Security Guard, Synergi Fusion RP; flow 0.8 mL/min; mobile phase A, 0.1% HCOOH Millipore grade; mobile phase B, MeCN LC-MS grade; 10% B to 40% B in 2 min; 40% B to 100% B in 1.5 min; 100% B for 1.5 min. Accurate mass spectrometric analysis was performed on an LTQ Orbitrap XL mass spectrometer (Thermo Electron, Bremen, Germany). For the analysis, a 5 μM solution of the corresponding sample in water/MeCN (50/50, 0.1%

formic acid) was directly injected via the syringe pump with a flow rate of 1 μL/min. The singly charged polydimethylcyclosiloxane background ion $(Si(CH_3)_2O)_6H^+$ (m/z 445.120025) generated during the electrospray process from ambient air was used as lock mass for real time internal recalibration. Further mass spectrometric settings were as follows: spray voltage was set to 1.6 kV, temperature of the heated transfer capillary was set to 200 °C. MS spectra (from m/z 400−2000) were acquired in the orbitrap with a resolution of r = 60000 at m/z 400 (after accumulation to a target value of 500000 charges in the linear ion trap). Proton nuclear magnetic resonance (^{1}H NMR) spectra and carbon nuclear magnetic resonance (^{13}C NMR) spectra were recorded on an Avance 400 (400 MHz) spectrometer from Bruker. Chemical shifts are reported in ppm relative to $CHCl_3$ (δ 7.26) for ^{1}H NMR and the central resonance of $CDCl_3$ (δ 77.0) for ^{13}C NMR. The purity of compounds (≥95%) was confirmed by elution as a single peak by LCT and NMR spectra. The synthesis of the capture compound scaffolds[19] **4**, **9**, and **10** is published elsewhere.[12]

Capture Compound 5. A solution of **1** (34.0 mg, 72 μmol) and scaffold X-NH-C_4H_8-NH_2 (73.0 mg, 87 μmol) in dry DMA (10 mL) was treated with DIPEA (63 μL, 361 μmol), HOBt (16.6 mg, 108 μmol), DMAP (44.0 mg, 361.0 μmol), and DCC (22.3 mg, 108 μmol). The reaction mixture was stirred for 17 h at 50 °C with exclusion of light. The solvent was removed under reduced pressure, and the crude product was directly purified by MPLC (eluent A, 0.1% AcOH; eluent B, MeCN; 20% B to 50% B in 20 min) to yield a pure fraction of **5** (52.0 mg, 40 μmol, 56%). ^{1}H NMR (400 MHz, MeOD): δ (ppm) = 8.36 (ddd, J = 4.9, 1.9, and 0.8 Hz, 1H), 7.93/7.32 (AA′BB′, J = 8.5 Hz, 4H), 7.61/6.85 (AA′BB′, J = 8.9 Hz, 4H), 7.58 (dd, J = 1.5 and 0.6 Hz, 1H), 7.53 (ddd, J = 8.1, 7.5, and 1.9 Hz, 1H), 7.37 (dd, J = 8.5 and 0.6 Hz, 1H), 7.21 (dd, J = 8.5 and 1.5 Hz, 1H), 7.12 (ddd, J = 7.5, 4.9, and 0.8 Hz, 1H), 6.97 (dt, J = 8.1 and 0.8 Hz, 1H), 4.9 (m below H_2O signal), 4.69 (br, s, 2H), 4.47 (ddd, J = 7.8, 4.9, and 0.8 Hz, 1H), 4.34 (t, J = 7.0 Hz, 2H), 4.29 (dd, J = 7.9 and 4.5 Hz, 1H), 3.82 (s, 3H), 3.61−3.52 (m, 8H), 3.50 (t, J = 6.1 Hz, 2H), 3.49 (t, J = 6.1 Hz, 2H), 3.27 (t, J = 6.8 Hz, 2H), 3.24 (t, J = 6.8 Hz, 2H), 3.18 (ddd, J = 8.9, 5.7 and 4.5, 1H), 3.17−3.13 (m, 2H), 3.10−3.05 (m, 2H), 2.91 (dd, J = 12.7 and 4.9 Hz, 1H), 2.77 (dd, J = 14.9 and 5.8 Hz, 1H), 2.70 (dd, J = 14.9 and 7.8 Hz, 1H), 2.69 (br d, J = 12.4 Hz, 1H), 2.63 (t, J = 6.8 Hz, 2H), 2.17 (t, J = 7.4 Hz, 2H), 1.77−1.52 (m, 8H), 1.50−1.37 (m, 6H). ^{13}C NMR (100.6 MHz, MeOD): δ (ppm) = 175.9, 173.4, 173.2, 172.9, 172.3, 168.4, 167.2, 166.1, 157.4, 155.1, 154.7, 149.9, 141.8, 139.5, 138.7, 136.6, 133.4, 131.4, 130.7, 129.3, 127.7, 124.9, 124.3, 123.4 (q, J = 274.1 Hz), 123.1, 120.8, 115.7, 113.4, 110.8, 71.5, 71.5, 71.2, 71.2, 69.9, 69.9, 63.4, 61.6, 57.0, 52.7, 47.0, 41.1, 41.1, 40.1, 40.0, 38.5, 38.1, 37.8, 36.8, 35.8, 30.6, 30.4, 30.3, 29.8, 29.5, 29.5 (q, J = 41.2 Hz), 27.7, 27.6, 26.9. LCT method B: t_R = 3.15 min; calcd for $C_{62}H_{80}F_3N_{16}O_{10}S$ $[MH]^+$, 1297.59106; obsd, 1298.2 (75%); 649.6 (100%). HRMS: obsd, 1297.58853 (−1.9 ppm).

Capture Compound 6. At 0 °C, a solution of compound **12** (1.0 mg, 0.75 μmol) in a solvent mixture of THF and water (15 μL, 2/1 v/v) was treated with a solution of lithium hydroxide (0.054 mg, 2.3 μmol) in water. The reaction mixture was stirred for 17 h at 4 °C. At 0 °C, the pH was adjusted to 4 by addition of diluted acetic acid solution. The crude product was directly purified by HPLC (eluent A, 0.1% HCOOH; eluent B, MeCN; 10% B for 7 min; 10% B to 100% B in 1 min; 100% B for 16 min) to give **6** (0.47 mg, 0.36 μmol, 48%). ^{1}H NMR (400 MHz, MeOD): δ (ppm) = 8.34 (ddd, J = 4.9, 1.9, and 0.7 Hz, 1H), 7.93/7.31 (AA′BB′, J = 8.5 Hz, 4H), 7.59 (br s, 1H), 7.55 (td, J = 7.6 and 1.9 Hz, 1H), 7.49/6.83 (AA′BB′,J = 8.8, 4H), 7.35 (br d, J = 8.5 Hz, 1H), 7.29 (dd, J = 8.5 and 1.5 Hz, 1H), 7.12 (ddd, J = 7.5, 4.9, and 0.9 Hz, 1H), 7.06 (dt, J = 8.1 and 0.8 Hz, 1H), 4.9 (m below H_2O signal), 4.68 (br s, 2H), 4.47 (ddd, J = 7.9, 5.0, and 0.8 Hz, 1H), 4.33−4.27 (m, 3H), 3.82 (s, 3H), 3.60−3.50 (m, 8H), 3.49 (t, J = 6.1 Hz, 2H), 3.47 (t, J = 6.1 Hz, 2H), 3.39−3.33 (m, 2H), 3.27−3.21 (m, 6H), 3.18 (ddd, J = 8.9, 5.8, and 4.5 Hz, 1H), 2.90 (dd, J = 12.8 and 5.0 Hz, 1H), 2.83 (dd, J = 14.9 and 6.0 Hz, 1H), 2.69 (dd, J = 14.9 and 7.5 Hz, 1H), 2.69 (br d, J = 12.6 Hz, 1H), 2.63−2.57 (m, 2H), 2.17 (t, J = 7.4 Hz, 2H), 1.76−1.52 (m, 12H), 1.46−1.37 (m, 2H). ^{13}C NMR (100.6 MHz, MeOD): δ (ppm) = 178.7, 175.9, 173.1, 172.8, 172.7, 168.5, 166.1, 164.9, 157.5, 155.0, 154.1, 149.9, 141.8, 139.5, 138.5, 136.6, 133.4, 131.9, 130.5, 129.4, 127.7, 124.8, 124.4, 123.1, 120.6, 117.1, 113.5, 110.7, 71.5, 71.4, 71.2, 71.2, 69.9, 63.4, 61.6, 57.0, 52.7, 48.0, 43.6, 41.2, 41.1, 39.6, 38.7, 38.2, 37.9, 37.2, 36.8, 30.6, 30.4, 30.3, 29.8, 29.5, 27.9, 26.9, 26.0. LCT method B: t_R = 3.12 min; calcd for $C_{62}H_{79}F_3N_{15}O_{11}S$ $[MH]^+$, 1298.57508; obsd, 1299.2 (20%); 650.1 (100%). HRMS: obsd, 1298.57603 (+0.7 ppm).

Capture Compound 7. At 0 °C, a solution of **3** (5.0 mg, 12 μmol) and scaffold X-NH-C_4H_8-NH_2 (9.3 mg, 11 μmol) in dry DMA (0.3 mL) was treated with DIPEA (9.7 μL, 55 μmol) and HATU (4.64 mg, 12 μmol). The reaction solution was stirred for 10 min at 0 °C, was allowed to warm to 23 °C, and was stirred additionally 17 h with exclusion of light. As LCT indicated incomplete conversion, HATU (1.9 mg, 5 μmol) and **3** (1.0 mg, 2 μmol) were added and stirring was continued for 17 h with exclusion of light. The solvent was removed under reduced pressure, and the crude product was directly purified by MPLC (eluent A, 0.1% AcOH; eluent B, MeCN; 0% B to 45% B in 20 min) to yield a pure fraction of **7** (9.3 mg, 7 μmol, 67%) as a colorless solid. ^{1}H NMR (400 MHz, MeOD): δ (ppm) = 7.95/7.36 (AA′BB′, J = 8.3 Hz, 4H), 7.76/7.57 (AA′BB′, J = 8.5 Hz, 4H), 4.9 (m below H_2O signal, C(x)-*H*), 4.8 (m below H_2O signal, C(x)-*H*), 4.63/4.47 (AB, J = 15.9 Hz, 2H), 4.49 (ddd, J = 7.7, 5.0, and 0.9 Hz, 1H), 4.30 (dd, J = 7.9 and 4.4 Hz, 1H), 4.32−4.28 (m, 2H), 3.62−3.53 (m, 8H), 3.52−3.49 (m, 4H), 3.35−3.12 (m, 9H), 3.19/3.08 (AB, J = 16.1 Hz, 2H), 2.94 (dd, J = 6.5 and 1.3 Hz, 1H), 2.92 (dd, J = 12.5 and 4.9 Hz, 1H), 2.80 (dd, J = 14.9 and 6.0 Hz, 1H), 2.70 (br d, J = 12.5 Hz, 1H), 2.69 (dd, J = 14.9 and 7.6 Hz, 1H), 2.59 (dtd, J = 11.4, 9.4, and 6.3 Hz, 1H), 2.31 (ddt, J = 11.5, 9.4, and 5.7 Hz, 1H), 2.18 (t, J = 7.4 Hz, 2H), 2.00 (br d, J = 12.5 Hz, 1H), 1.90 (s, 3H), 1.83−1.38 (m, 19H), 1.33−1.14 (m, 4H), 1.05 (m, 1H). ^{13}C NMR (100.6 MHz, MeOD): δ (ppm) = 176.1, 176.0, 174.1, 173.0, 172.9, 172.3, 168.4, 166.1, 146.9, 136.6, 133.4, 129.4, 129.2, 129.1, 127.7, 71.5, 71.5, 71.2, 71.2, 70.0, 69.9, 63.5, 63.4, 62.6, 61.6, 57.0, 52.7, 51.5, 50.4, 43.6, 42.0, 41.1, 40.0, 39.7, 38.5, 38.2, 37.9, 36.9, 30.9, 30.4, 30.3, 29.8, 29.5, 27.8, 27.7, 27.5, 27.3, 27.2, 26.9. LCT method B: t_R = 3.05 min; calcd for $C_{59}H_{86}F_3N_{14}O_{11}S$ $[MH]^+$, 1255.62678; obsd, 1256.2 (15%); 628.6 (100%). HRMS: obsd, 1255.62629 (−0.4 ppm).

Capture Compound 8. At 0 °C, a solution of compound **17** (8.6 mg, 7 μmol) in a solvent mixture of THF and water (1.5 mL, 1/1 v/v) was treated with lithium hydroxide (0.49 mg, 20 μmol). The reaction mixture was stirred for 1 h at 0 °C. THF (1.5 mL) was added, and the pH was adjusted to 7 by addition of 2 M HCl_{aq} at 0 °C. The solvents were removed under reduced pressure, and the crude product was directly purified by MPLC (eluent A, 0.1% AcOH; eluent B, MeCN; 10% B to 40% B in 5 min; 40% B for 7 min) to give **8** (6.6 mg, 5 μmol, 78%). ^{1}H NMR (400 MHz, MeOD): δ (ppm) = 7.95/7.33 (AA′BB′, J = 8.5 Hz, 4H), 7.77/7.42 (AA′BB′, J = 8.2 Hz, 4H), 4.9 (m below H_2O signal), 4.8 (m below H_2O signal), 4.53/4.46 (AB, J = 15.5 Hz, 2H), 4.48 (ddd, J = 7.9, 5.0, and 0.7 Hz, 1H), 4.37 (td, J = 9.0 and 6.4 Hz, 1H), 4.29 (dd, J = 7.9 and 4.5 Hz, 1H), 4.23 (td, J = 9.0 and 5.6 Hz, 1H), 3.62−3.53 (m, 8H), 3.51 (t, J = 6.2 Hz, 2H), 3.50 (t, J = 6.0 Hz, 2H), 3.40−3.20 (m, 11H), 3.18 (m, 1H), 2.91 (dd, J = 12.8 and 5.0 Hz, 1H), 2.79 (dd, J = 14.8 and 5.9 Hz, 1H), 2.72 (dd, J = 14.8 and 7.9 Hz, 1H), 2.70 (br d, J = 12.7 Hz, 1H), 2.62 (dtd, J = 11.4, 9.2, and 6.4 Hz, 1H), 2.31 (ddt, J = 11.4, 9.2, and 5.6 Hz, 1H), 2.18 (t, J = 7.4 Hz, 2H), 1.90 (br d, J = 12.4 Hz, 1H), 1.86−1.51 (m, 17H), 1.46−1.36 (m, 2H), 1.33−1.11 (m, 4H), 1.06 (m, 1H). ^{13}C NMR (100.6 MHz, MeOD): δ (ppm) = 176.0, 175.1, 173.0, 172.3, 172.2, 170.0, 168.5, 166.1, 161.6, 143.6, 136.6, 134.6, 133.4, 129.4, 128.6, 128.5, 127.7, 71.5, 71.5, 71.2, 71.2, 70.0, 69.9, 63.4, 63.0, 62.4, 61.6, 57.0, 52.8, 50.7, 43.8, 41.1, 40.9, 40.5, 40.1, 38.6, 38.2, 37.9, 36.9, 30.4, 30.3, 29.9, 29.8, 29.8, 29.5, 27.7, 27.0, 26.9. LCT method B: t_R = 3.42 min; calcd for $[MH]^+$, 1257.59481; obsd, 1258.2 (100%); 629.6 (30%). HRMS: obsd, 1257.59488 (−0.055 ppm).

Ethyl 3-(2-((4-(*N*-(4-(*tert*-Butoxycarbonylamino)butyl)-carbamimidoyl)phenylamino)methyl)-1-methyl-*N*-(pyridin-2-yl)-1*H*-benzo[*d*]imidazole-5-carboxamido)propanoate (11). In a screw top vial, a solution of dabigatran ethyl ester acetate (10.0 mg, 18 μmol) (from Suzhou Unite PharmTech Co.) in dry EtOH (25 μL) was treated with *tert*-butyl 4-aminobutylcarbamate (33.6 mg, 180 μmol). The vial was tightly screwed, and the reaction mixture was

stirred at 78 °C for 12 h. As LCT analyses showed almost complete conversion, the solvent was removed by argon stream and the crude product was directly purified by MPLC (eluent A, 0.1% AcOH; eluent B, MeCN; 30% B to 40% B in 6 min; 40% B for 4 min) to give desired product **11** (10.9 mg, 16 μmol, 91%) as a colorless solid. ^{1}H NMR (400 MHz, MeOD): δ (ppm) = 8.39 (dd, *J* = 5.0 and 1.8 Hz, 1H), 7.57 (br d, *J* = 1.2 Hz, 1H), 7,52 (m, 1H), 7.52/6.84 (AA′BB′, *J* = 8.8 Hz, 4H), 7.37 (d, *J* = 8.5 Hz, 1H), 7.28 (dd, *J* = 8.4 and 1.3 Hz, 1H), 7.14 (dd, *J* = 7.3 and 5.0 Hz, 1H), 6.93 (d, *J* = 8.0 Hz, 1H), 4.68 (br s, 2H), 4.36 (t, *J* = 7.0 Hz,2H), 4.05 (q, *J* = 7.1 Hz, 2H), 3.82 (s, 3H), 3.40 (t, *J* = 7.2 Hz, 2H), 3.09 (t, *J* = 6.9 Hz, 2H), 2.75 (t, *J* = 7.0 Hz, 2H), 1.75−1.67 (m, 2H), 1.61−1.54 (m, 2H), 1.43 (s, 9H), 1.20 (t, *J* = 7.2 Hz, 3H). ^{13}C NMR (100.6 MHz, MeOD): δ (ppm) = 173.2, 173.1, 165.1, 158.8, 157.3, 155.2, 154.1, 150.0, 141.8, 139.4, 138.7, 131.3, 130.4, 124.9, 124.4, 123.1, 120.7, 117.3, 113.4, 110.7, 80.0, 61.8, 46.2, 43.6, 41.2, 40.5, 34.1, 30.6, 28.8, 28.5, 26.1, 14.4. LCT method B: t_R = 3.16 min, calcd for $C_{36}H_{47}N_8O_5$ [MH] $^+$, 671.36639; obsd, 671.6 (80%). HRMS: obsd, 671.36462 (−2.6 ppm).

Compound 12. At 0 °C, a solution of compound **11** (10.0 mg, 15 μmol) in dry DCM (1.0 mL) was treated with TFA (0.2 mL) and stirred at 0 °C for 1 h. All volatile materials were removed under reduced pressure. The crude product was coevaporated twice with DCM, dried under high vacuum, and dissolved in dry DMA (0.3 mL). At 0 °C, the solution was successively treated with scaffold X−OH (13.8 mg, 18.0 μmol), DIPEA (26 μL, 15 μmol), and HATU (6.2 mg, 16 μmol). The reaction mixture was stirred for 10 min at 0 °C, was allowed to warm to 23 °C, and was stirred for additional 2 d with exclusion of light. The solvent was removed under reduced pressure, and the crude product was directly purified by MPLC (eluent A, 0.1% AcOH; eluent B, MeCN; 30% B to 45% B in 9 min; 45% B for 3 min) to yield **12** (6.9 mg, 5 μmol, 35%). ^{1}H NMR (400 MHz, MeOD): δ (ppm) = 8.39 (ddd, *J* = 4.9, 1.9, and 0.7 Hz, 1H), 7.92/7.31 (AA′BB′, *J* = 8.4 Hz, 4H), 7.58 (dd, *J* = 1.5 and 0.6 Hz, 1H), 7.51 (ddd, *J* = 8.1, 7.6, and 1.9 Hz, 1H), 7.49/6.83 (AA′BB′, *J* = 8.9 Hz, 4H), 7.37 (dd, *J* = 8.5 and 0.6 Hz, 1H), 7.28, *J* = 8.5 and 1.5 Hz, 1H), 7.13 (ddd, *J* = 7.5, 4.9, and 0.8 Hz,1H), 6.93 (dt, *J* = 8.0 and 0.8 Hz,1H), 4.92 (dd, *J* = 5.8 and 1.5 Hz, 1H), 4.68 (br s, 2H), 4.47 (ddd, *J* = 7.8, 4.9, and 0.8 Hz, 1H), 4.36 (t, *J* = 7.0 Hz, 2H), 4.28 (dd, *J* = 7.8 and 4.4 Hz, 1H), 4.05 (q, *J* = 7.1 Hz, 2H), 3.83 (s, 3H), 3.60−3.50 (m, 8H), 3.49 (t, *J* = 6.1 Hz, 2H), 3.47 (t, *J* = 6.1 Hz, 2H), 3.39−3.35 (m, 2H), 3.27−3.21 (m, 6H), 3.18 (ddd, *J* = 9.0, 5.8, and 4.5 Hz,1H), 2.91 (dd, *J* = 12.8 and 4.9 Hz,1H), 2.83 (dd, *J* = 14.9 and 6.1 Hz,1H), 2,75 (t, *J* = 7.0 Hz,2H), 2.68 (dd, *J* = 14.8 and 7.4 Hz, 1H), 2.68 (br d, *J* = 12.8 Hz, 1H), 2.17 (t, *J* = 7.4 Hz, 2H), 1.78−1.49 (m, 12H), 1.46−1.37 (m, 3H), 1.20 (t, *J* = 7.2 Hz,3H). ^{13}C NMR (100.6 MHz, MeOD): δ (ppm) = 175.9, 173.2, 173.1, 172.8, 172.7, 168.4, 166.1, 164.9, 157.3, 155.2, 154.1, 150.0, 141.8, 139.5, 138.7, 136.6, 133.4, 131.3, 130.5, 129.3, 127.7, 124.9, 124.4, 123.1, 120.7, 117.1, 113.4, 110.8, 71.5, 71.4, 71.2, 71.2, 69.9, 63.4, 61.8, 61.6, 57.0, 52.6, 46.2, 43.6, 41.2, 41.0, 39.5, 38.6, 38.2, 37.9, 36.9, 34.1, 30.7, 30.4, 30.3, 29.8, 29.5, 27.9, 26.9, 26.0, 14.4. LCT method B: t_R = 3.34 min; calcd for $C_{64}H_{83}F_3N_{15}O_{11}S$ [MH]$^+$, 1326.60638; obsd, 1327.2 (50%), 664.1 (100%). HRMS: obsd, 1326.60599 (−0.3 ppm).

***tert*-Butyl 4-(4-(4-Nitrophenylsulfonamido)butylcarbamoyl)-benzylcarbamate (14).** A solution of 4-(*tert*-butoxycarbonylamino-methyl)-benzoic acid (1.0 g, 3.98 mmol) in dry DMA (30 mL) was treated with DIPEA (3.47 mL, 19.9 mmol) and HATU (1.59 g, 4.18 mmol). After stirring for 2 min, a solution of *N*-(4-aminobutyl)-4-nitrobenzenesulfonamide (1.54 g, 3.98 mmol) in dry DMA (10 mL) and DMAP (486 mg, 3.98 mmol) were added and the reaction mixture was stirred for 1.5 h at 23 °C. DCM (250 mL) was added, and the organic layer was washed with brine (2 times 100 mL). The organic layer was dried over $MgSO_4$, the solvents were removed under reduced pressure, and the crude product was recrystallized from pure DCM to yield compound **14** (1.72 g, 3.38 mmol, 85%) as a colorless solid. ^{1}H NMR (400 MHz, DMSO-*d*): δ (ppm) = 8.40/8.03 (br AA′BB′, *J* = 8.4 Hz, 4H), 8.35 (br s, 1H), 7.98 (br s, 1H), 7.74/7.28 (br AA′BB′, *J* = 7.4 Hz, 4H), 7.44 (br s, 1H), 4.16 (br d, 2H), 3.18 (br q, 2H), 2.82 (br q, 2H), 1.52 −1.28 (m, 13H). ^{13}C NMR (100.6 MHz, DMSO-*d*): δ (ppm) = 165.9, 155.8, 149.5, 146.2, 143.3, 133.0, 128.0, 127.1, 126.6, 124.6, 77.9, 43.1, 42.3, 38.5, 28.2, 26.6, 26.2. LCT method B: t_R = 3.85 min; calcd for $C_{23}H_{31}N_4O_7S$ [MH]$^+$, 507.19080; obsd, 507.4 (20%); 451.3 (100%). HRMS: obsd, 507.19043 (−0.73 ppm).

***tert*-Butyl (*S*)-1-Cyclohexyl-2-((*R*)-2-(4-(4-(4-nitrophenylsulfonamido)butylcarbamoyl)benzylcarbamoyl)-azetidin-1-yl)-2-oxoethylcarbamate (15).** At 0 °C, a suspension of compound **14** (858 mg, 1.69 mmol) in a solvent mixture of DCM and MeOH (18 mL, 1/1 v/v) was treated with TFA (4 mL). The reaction mixture was stirred at 0 °C for 1 h, was allowed to warm to 23 °C, and was stirred additionally 2 h at 40 °C. As LCT indicated full conversion, all volatile materials were removed under reduced pressure. The crude product was coevaporated twice with DCM, dried under high vacuum, and dissolved in dry DMA (0.2 mL). At 0 °C, this solution was added dropwise to a solution of (*S*)-1-((*R*)-2-(Boc-amino)-2-cyclohexylacetyl)azetidine-2-carboxylic acid (576 mg, 1.69 mmol), DIPEA (2.95 mL, 16.9 mmol), and HATU (708 mg, 1.86 mmol) in dry DMA (0.2 mL). The reaction mixture was stirred for 5 min at 0 °C, was allowed to warm to 23 °C, and was stirred for additional 2 d with exclusion of light. The solvent was removed under reduced pressure, and the crude product was directly purified by column chromatography (eluent A, DCM; eluent B, MeOH; 1% B to 4% B) to yield **15** (1.18 g, 1.62 mmol, 96%) as a colorless foam. ^{1}H NMR (400 MHz, $CDCl_3$): δ (ppm) = 8.29/8.03 (AA′BB′, *J* = 8.7 Hz, 4H), 8.25 (br t, *J* = 6 Hz, 1H), 7.64/7.25 (AA′BB′, *J* = 8 Hz,4H), 6.9 (br s, 1H), 6.27 (br t, *J* = 5.7 Hz, 1H), 5.16 (br d, *J* = 5 Hz, 1H), 4.86 (dd, *J* = 9.0 and 5.7 Hz, 1H), 4.57 (dd, *J* = 15.6 and 6.3 Hz, 1H), 4.42 (td, *J* = 8.4 and 5.8 Hz, 1H), 4.32 (dd, *J* = 15.7 and 5.1 Hz, 1H), 4.18 (td, *J* = 8.5 and 5.7 Hz, 1H), 3.77 (t, *J* = 7.6 Hz, 1H), 3.36−3.26 (m, 2H), 2.99−2.91 (m, 2H), 2.64 (m, 1H), 2.44 (m, 1H), 1.83 (br d, *J* = 12.2 Hz, 1H), 1.80−1.44 (m, 9H), 1.30 (s, 9H), 1.26−0.96 (m, 5H). ^{13}C NMR (100.6 MHz, $CDCl_3$): δ (ppm) = 172.9, 171.3, 168.4, 156.3, 150.0, 146.3, 142.4, 132.8, 128.4, 127.5, 127.2, 124.4, 80.4, 61.8, 55.3, 48.9, 43.1, 42.9, 39.9, 39.5, 29.7, 29.1, 28.4, 26.7, 26.0, 25.9, 20.3. LCT method A: t_R = 10.88 min; calcd for $C_{35}H_{49}N_6O_9S$ [MH]$^+$, 729.32762; obsd, 729.0 (5%); 629.0 (100%). HRMS: obsd, 729.32700 (−0.85 ppm).

Methyl 2-((*S*)-1-Cyclohexyl-2-((*R*)-2-(4-(4-(4-nitrophenylsulfonamido)butylcarbamoyl)benzylcarbamoyl)-azetidin-1-yl)-2-oxoethylamino)acetate (16). At 0 °C, a solution of compound **15** (250 mg, 343 μmol) in dry DCM (20 mL) was treated with TFA (5 mL) and stirred for 30 min at 0 °C. As TLC indicated full conversion, all volatile materials were removed under reduced pressure. The crude product was coevaporated twice with DCM and dried under high vacuum. Under an atmosphere of argon, the crude product was dissolved in dry MeCN (17 mL) and treated with methyl 2-(4-nitrophenylsulfonyloxy)acetate (113 mg, 412 μmol) and potassium carbonate (119 mg, 858 μmol). The reaction mixture was stirred at 60 °C. After 30 min, additional methyl 2-(4-nitrophenylsulfonyloxy)acetate (113 mg, 412 μmol) was added and stirring was continued for 1 h. The solvent was removed under reduced pressure, and the crude product was directly purified by column chromatography (eluent A, DCM; eluent B, MeOH; 1% B to 10%) to yield compound **16** as a nonpure product (168 mg) which was used as such for the next step. LCT method A: t_R = 6.37 min; calcd for $C_{33}H_{45}N_6O_9S$ [MH]$^+$, 701.29632; obsd, 701.2 (100%).

Compound 17. Under an atmosphere of argon, a solution of compound **16** (108 mg, 154 μmol) in dry MeCN (5 mL) was treated with 2-mercaptoacetic acid (32.1 μL, 462 μmol) and DBU (116 μL, 771 μmol) and was stirred at 0 °C for 1 h. All volatile materials were removed under reduced pressure, and the crude product was enriched via MPLC (eluent A, 0.1% AcOH; eluent B, MeCN; 10% B to 40% B in 30 min). All product containing fractions were combined, and the solvents were removed under reduced pressure. The crude product was dissolved in dry DMA (0.3 mL) and treated with scaffold X−OH (27.2 mg, 35 μmol), DIPEA (55 μL, 320 μmol), and HATU (13.4 mg, 35 μmol). The reaction mixture was stirred for 10 min at 0 °C, was allowed to warm to 23 °C, and was stirred additionally 17 h with exclusion of light. The solvent was removed under reduced pressure and the crude product was directly purified by MPLC (eluent A, 0.1% AcOH; eluent B, MeCN; 10% B to 60% B in 30 min) to yield

dx.doi.org/10.1021/jm3001339 | *J. Med. Chem.* 2012, 55, 3934−3944

compound **17** (17.4 mg, 15 μmol, 43%) as a colorless solid. ^{1}H NMR (400 MHz, MeOD): δ (ppm) = 7.94/7.34 (AA′BB′, *J* = 8.5 Hz, 4H), 7.77/7.41 (AA′BB′, *J* = 8.2 Hz, 4H), 4.9 (m below H_2O signal), 4.81 (dd, *J* = 9.4 and 5.6 Hz, 1H), 4.53/4.47 (AB, *J* = 15.7 Hz, 2H), 4.48 (dd, *J* = 7.7 and 5.0, 1H), 4.29 (dd, *J* = 7.8 and 4.5 Hz, 1H), 4.31−4.18 (m, 2H), 3.64 (s, 3H), 3.61−3.52 (m, 8H), 3.50 (t, *J* = 6.2 Hz, 2H), 3.50 (t, *J* = 6.0 Hz, 2H), 3.37−3.16 (m, 11H), 3.08 (d, *J* = 7.4 Hz, 1H), 2.91 (dd, *J* = 12.7 and 4.9 Hz, 1H), 2.80 (dd, *J* = 14.9 and 5.9 Hz, 1H), 2.72 (dd, *J* = 14.9 and 7.6 Hz, 1H), 2.70 (br d, *J* = 12.7 Hz, 1H), 2.60 (dtd, *J* = 11.4, 9.2, and 6.5 Hz, 1H), 2.28 (ddt, *J* = 11.4, 9.2, and 5.7 Hz, 1H), 2.18 (t, *J* = 7.4 Hz, 2H), 1.96 (br d, *J* = 12.7 Hz, 1H), 1.81−1.51 (m, 17H), 1.46−1.38 (m, 2H), 1.32−1.12 (m, 4H), 1.04 (m, 1H). ^{13}C NMR (100.6 MHz, MeOD): δ (ppm) = 175.9, 175.8, 174.2, 172.9, 172.7, 172.3, 169.8, 168.4, 166.1, 143.5, 136.6, 134.6, 133.4, 129.3, 128.6, 128.5, 127.7, 123.4 (q, *J* = 274.1 Hz), 71.5, 71.5, 71.2, 71.2, 69.9, 69.9, 63.4, 62.9, 62.5, 61.6, 57.0, 52.7, 52.3, 50.3, 43.7, 42.1, 41.1, 40.5, 40.1, 38.5, 38.1, 37.8, 36.8, 30.6, 30.4, 30.3, 29.8, 29.5 (q, *J* = 40.6 Hz), 29.5, 27.8, 27.4, 27.3, 27.2, 26.9. LCT method B: t_R = 3.27 min; calcd for $C_{60}H_{86}F_3N_{12}O_{13}S$ $[MH]^+$, 1271.61046; obsd, 1272.0 (75%); 636.5 (100%). HRMS: obsd, 1271.60929 (−0.92 ppm).

Stability Tests for the Capture Compounds. The stability of all CCs was evaluated for the following conditions: thermal stress (incubation of CC native or denatured for 30 min at 4 and 80 °C respectively) and biological stress (incubation of CC in HepG2 cell lysates for 30 min at 4 and 37 °C, respectively). Moreover, it was determined that after UV irradiation for 10 and 30 min in the caproBox, only one defined reaction product is formed. The caproBox is a device that enables controlled UV irradiation with simultaneous cooling. The characteristics of the caproBox are as follows: capture temperature 0.5−4 °C, λ = 275−375 nm with λ_{max} = 312 nm, irradiance I_e 10−12 mW/cm^2, irradiation energy for each sample ca. 1 J. No degradation of the CC was observed when it was exposed under normal overhead light for 1 h. The protocol for the experimental determination of stability has been published.[36]

Cell Lysates. The HepG2 and K562 cell lines were purchased from the German collection of microorganisms and cell lines (DSMZ, Braunschweig, Germany) and cultivated according to the provided instructions. The protocol for the preparation of cell lysates has been described elsewhere.[13]

CCMS Experiments. Protein concentrations were determined according to Bradford.[37] Protein input material was either 400 μg of HepG2 or K562 cell lysate (400 μg) or 1 μg of human recombinant NQO2 (Sigma Aldrich, Germany) or 2 μg of human recombinant thrombin (Sigma Aldrich, Germany). The protein input was supplemented with 20 μL of 5× capture buffer (caprotec bioanalytics GmbH, Berlin, Germany). In the case of cell lysates, a preclearing step was then carried out: beads from 50 μL streptavidin coated DynaBead-Suspension (Invitrogen) slurry were added, incubated for 30 min at 4 °C, and removed to reduce naturally biotinylated proteins from the lysates. For the competition control, additional 10 μL of a 1 mM solution of either **1**, **2**, **3**, or **4** was added and the reaction volumes of both the capture reaction and competition control were adjusted to 90 μL with Milli-Q water and incubated for 30 min at 4 °C on a rotation wheel. A solution of either one of the CCs **5** or **6**, CCs **7** or **8**, or CCs **9** and **10** (10 μL of a 50 μM solution) were added to the capture, and respective competition experiments and equilibration was carried out for 1 h at 4 °C. Then the reaction mixture was irradiated for 10 min using the caproBox. Subsequently, buffer conditions were adjusted by adding 25 μL of 5× wash buffer (caprotec bioanalytics GmbH, Berlin, Germany) to each reaction. The samples were then incubated with 50 μL Dynabeads MyOne Streptavidin C1, (Invitrogen, Karlsruhe, Germany) for 1 h at 4 °C on a rotation wheel. The beads containing the CC−protein conjugates were then collected using the caproMag, a device for the convenient handling of magnetic beads (caprotec bioanalytics GmbH, Berlin, Germany), and washed first six times with 200 μL 1× WB, then three times with 80% MeCN and finally once with MS grade water. MeCN was used to remove polymers from the beads. The beads were stored at 4 °C in deionized water until further analysis by either SDS-PAGE or protein digestion followed by LC-MS analysis.

Silver Stained SDS-PAGE and Western Blots. were carried out according to the standard laboratory procedures as published previously.[13] For silver staining, the ProteoSilver Kit (Sigma Aldrich, Germany) was used according to the manufacturer's instructions. Antibodies were diluted as follows: anti-NQO2 1:500 (abcam, Cambridge, UK) and secondary antirabbit antibody conjugated to horseradish peroxidase 1:1000 (abcam, Cambridge, UK). In the case of blots for the detection of biotinylated proteins, streptavidin−horseradish peroxidase (Sigma Aldrich, Germany) was used instead of a first antibody at a dilution of 1:1000 and blots were developed directly after washing. Intensity of gel bands was determined using the ImageJ software (Wayne Rasband, National Institues of Health, USA, http://rsb.info.nih.gov/ij/freeware).

Protein Digestion. After protein capturing, streptavidin magnetic beads were washed twice with 200 μL of LC-MS grade water (Fluka, St. Louis, MO, USA). For tryptic digestion, the proteins bound to the streptavidin magnetic beads were incubated with 9 μL of 50 mM ammonium bicarbonate and 1 μL of trypsin (0.5 μg/μL) (Roche, Germany) for 16 h at 37 °C on a temperature-controlled shaker. The supernatant was removed and evaporated to dryness in a miVac DNA vacuum centrifuge (Genevac, UK) and stored at −20 °C until mass spectrometric analysis.

Mass Spectrometric Analysis. Tryptic digests were analyzed by an online nanoflow liquid chromatography system (nLC Proxeon, Biosystems, AIS, Denmark) connected to an LTQ Orbitrap XL mass spectrometer (Thermo Electron, Bremen, Germany) utilizing a nanoelectrospray ion source (Proxeon Biosystems A/S, Denmark). First, 5μL of the peptide solution were loaded directly onto a precolumn (nanoflow Biosphere C18, 5 μm, 120 Å, 20 mm × 0.1 mm; NanoSeparations, Netherlands) coupled to an analytical column (nanoflow Biosphere C18, 5 μm, 120 Å, 100 mm × 0.075 mm; NanoSeparations, Netherlands) using 5% MeCN/0.1% HCOOH. Then during the LC run, peptides were eluted during an 80 min linear gradient from 5% MeCN/0.1% HCOOH to 40% MeCN/0.1% HCOOH followed by an additional 2 min to 100% MeCN/0.1% HCOOH and remaining at 100% MeCN/0.1% HCOOH for another 8 min with a controlled flow rate of 400 nL/min. The LC-MS analysis was performed in the data-dependent mode to automatically switch between orbitrap-MS (profile mode) and LTQ-MS/MS (centroid mode) acquisition. The instrument was set to sequentially isolate the most intense ions (up to five, depending on signal intensity) for fragmentation in the linear ion trap using collision-induced dissociation (CID) at a target value of 10000 charges. The resulting fragment ions were recorded in the LTQ. Phosphorylation at serine, threonine, and tyrosine, oxidation of methionines, deamidation at asparagines and glutamine, acetylation at lysine and serine, formylation at lysine, and methylation at arginine, lysine, serine, threonine, and asparagine were allowed as variable modifications. No fixed modifications were used in the database search. Mass spectrometric settings: spray voltage to 1.6 kV, temperature of the heated transfer capillary 200 °C, and normalized collision energy is 35% for MS^2. The minimal signal required for MS^2 is 500 counts. An activation *q* = 0.25 and an activation time of 30 ms for MS^2 acquisitions was applied.

MS-Data Annotation and Analysis. MS data were analyzed using SEQUEST implemented in Bioworks Browser 3.3.1 SP1 (Thermo Fisher Scientific) and X!Tandem (www.thegpm.org, version 2007.01.01.1). Automated database search against the human UniProtKB/Swiss-Prot database (release 57.6) was performed with 5 ppm precursor tolerance, 1 Da fragment ions tolerance, and full trypsin specificity allowing for up to two missed cleavages. The estimated false discovery rate of peptide identifications was determined using the reversed protein database approach and was <0.5%. Only proteins identified with more than 99% probability and at least two unique peptides with 95% probability were considered to be identified with sufficient confidence. Furthermore, these protein hits were manually validated by inspection of the MS^2 spectra. For statistical analysis, Student's *t* test was carried out between the number of unweighted spectral counts in the four capture assays and the four competition controls. For the fold change, the average number of unweighted spectral counts in the assays was divided by the average number of

unweighted spectral counts in the competition control. We considered a protein to be significantly enriched in the capture assays compared to the competition controls if the fold change was greater than 2 and at the same time the *p*-value was smaller than 0.05 (corresponding to a negative $\log_{10}$ in the volcano plot of greater than 1.3, *y*-axis).

NQO2 Inhibition Assay. Using the NADH-dependent mitomycin C metabolism by NQO2, we examined **1** as a novel NQO2 inhibitor. NQO2 (0.5 μM) was incubated with the substrate mitomycin C (50 μM) and four different drug concentrations as indicated in 100 mM potassium phosphate buffer (pH 5.8) at room temperature for 5 min prior to the addition of NADH (in increasing concentrations) as a cosubstrate and photometric monitoring at 340 nm for 30 min at rt. Indicated amounts display final assay concentrations. We determined K_i values for different concentrations of **1** and **4** utilizing a Lineweaver–Burk application in Sigma Plot10. Data generated were used to calculate the IC_{50} of inhibition of NQO2 activity by **1**.

Thrombin Assay. The assay used to test for percent inhibition was a fluorescence assay utilizing Boc-Val-Pro-Arg-AMC, as first described by Morita et al.[38] and contracted to European ScreeningProt (Hamburg, Germany). The Boc-Val-Pro-Arg-AMC (15 μM) substrate in 5 μL of assay buffer assay buffer was supplemented with varying concentrations of either **1** or **2** (16 2-fold dilutions of compounds in DMSO, 2.5 mM to 75 nM). The assay buffer consisted of consisted of 50 mM Tris, pH 7.5, 150 mM NaCl, 0.05% Tween 20. Then α thrombin was added to a final concentration of 5.5 ng/mL and the reaction incubated for 2 h at room temperature. Subsequently, fluorescence was measured on an Envision reader (excitation 355 nm, emission 460 nm). Human α-thrombin was purchased from Haematilogic Technologies Inc. (HCT-0020). Substrate Boc-Val-Pro-Arg-AMC was from Bachem (I-1120.0050).

Molecular Docking. Coordinates were taken from the crystal structure of human QR2 in complex with resveratrol (PDB code 1SG0) and preprocessed with the SYBYL 8.1 Package. Hydrogens were added and minimized using the TRIPOS force field and Gasteiger–Marsili charges (rmsd = 0.1, structure A), followed by a staggered minimization protocol restraining (a) backbone, ligand, and Zn pocket (Zn, His-N and Cys-SH), (b) protein Cα atoms and Zn pocket, and (c) Zn pocket only (structure B). Docking studies were performed using Surflex-Dock[39] (SYBYL 8.1 or SYBYLX1.1.1, TRIPOS Inc., St. Louis, MO, USA). The resveratrol ligand was extracted and used for protomol generation. Structures of **1**, **2**, and truncated CCs **5** and **6** (Me and Et amides instead of the PEG-biotin moiety) were built, minimized (Tripos force field, Gasteiger–Marsili charges, rmsd = 0.05) and docked to the prepared protein (structures A and B). Docking was performed using the SurflexDock protocol with default parameters besides starting conformations (10) and number of resulting poses (50) or the SurflexGeom protocol with default parameters. All docking poses were collected and sorted in groups by orientation using an in-house script and evaluated by experimental criteria (binding of **1**, but not of **3**; Coplanar to FAD; open carboxyl terminus; amidine involved in ligand binding) and the docking scores.

■ ASSOCIATED CONTENT

Ⓢ Supporting Information

Additional computational results and figures and tables containing additional experimental data. This material is available free of charge via the Internet at http://pubs.acs.org.

■ AUTHOR INFORMATION

Corresponding Author

*Phone: +49 30 6392 3976. Fax: +49 30 6392 3985. E-mail: jenny.fischer@caprotec.com.

Present Address

[†]M.G.: Inovalab AG, Kägenstrasse 17, CH-4153 Reinach, Switzerland. R.M.: F. Hoffmann-La Roche Ltd., Bldg 52/r. 1108, Grenzacherstrasse 124, CH-4070 Basel, Switzerland.

Author Contributions

[‡]These authors contributed equally.

Notes

The authors declare no competing financial interest.

■ ACKNOWLEDGMENTS

We thank Philip Gribbon of European ScreeningPort GmbH, Hamburg, Germany, for experimental support in the thrombin assay.

■ ABBREVIATIONS USED

A, assay; Ac, acetyl; ACN, acetonitrile; Boc, *tert*-butyl carbamate; Asp, asparagine; C, competition; CC, capture compound; CCMS, capture compound mass spectrometry; CNS, central nervous system; DBU, 1,8-diazabicyclo[5.4.0]-undec-7-ene; DCC, *N*,*N*′-dicyclohexylcarbodiimide; DCM, dichloromethane; DIPEA, *N*,*N*-diisopropylethylamine; DMA, *N*,*N*-dimethylacetamide; DMAP, 4-dimethylaminopyridine; FAD, flavin adenine dinucleotide; FQ, fit quality of the ligand efficiency; HATU, *O*-(7-azabenzotriazol-1-yl)-*N*,*N*,*N*′,*N*′-tetramethyluronium hexafluoro-phosphate; HepG2, a human cell line derived from hepatocellular carcinoma; HOBt, 1-hydroxybenzotriazole; IC_{50}, concentration at which half the enzyme is inhibited; Ile, isoleucine; K562, a human cell line derived from myelogenous leukemia; K_i, the measure of bond-tightness between an enzyme and a corresponding enzyme inhibitor; LE, ligand efficiency; LTQ, linear trap quadrupole; Met, methionine; mRNA, messenger ribonucleic acid; NADH, nicotinamide adenine dinucleotide; NMR, nuclear magnetic resonance; NQO2, ribosyldihydronicotinamide dehydrogenase; *p*-value, probability value; PAGE, polyacrylamide gel electrophoresis; PEG, polyethylene glycol; Phe, phenylalanine; PI, isoelectric point; p*K*, negative logarithm of the dissociation constant; SAR, structure–activity relationship; SDS, sodium dodecylsulfate; TFA, trifluoroacetic acid; THF, tetrahydrofuran; UV, ultraviolet

■ REFERENCES

(1) Hopkins, A. L. Network pharmacology: the next paradigm in drug discovery. *Nature Chem. Biol.* **2008**, *4*, 682–690.

(2) Hopkins, A. L. Network pharmacology. *Nature Biotechnol.* **2007**, *25*, 1110–1111.

(3) Colinge, J.; Rix, U.; Bennett, K. L.; Superti-Furga, G. Systems biology analysis of protein–drug interactions. *Proteomics: Clin. Appl.* **2011**, *6*, 1–15.

(4) Yadav, P. N.; Abbas, A. I.; Farrell, M. S.; Setola, V.; Sciaky, N.; Huang, X. P.; Kroeze, W. K.; Crawford, L. K.; Piel, D. A.; Keiser, M. J.; Irwin, J. J.; Shoichet, B. K.; Deneris, E. S.; Gingrich, J.; Beck, S. G.; Roth, B. L. The presynaptic component of the serotonergic system is required for clozapine's efficacy. *Neuropsychopharmacology* **2011**, *36*, 638–651.

(5) Keiser, M. J.; Irwin, J. J.; Shoichet, B. K. The chemical basis of pharmacology. *Biochemistry* **2010**, *49*, 10267–10276.

(6) Cases, M.; Mestres, J. A chemogenomic approach to drug discovery: focus on cardiovascular diseases. *Drug Discovery Today* **2009**, *14*, 479–485.

(7) Brown, J. B.; Okuno, Y. Systems biology and systems chemistry: new directions for drug discovery. *Chem. Biol.* **2012**, *19*, 23–28.

(8) von Eichborn, J.; Murgueitio, M. S.; Dunkel, M.; Koerner, S.; Bourne, P. E.; Preissner, R. PROMISCUOUS: a database for network-based drug-repositioning. *Nucleic Acids Res.* **2011**, *39*, D1060–D1066.

(9) Hecker, N.; Ahmed, J.; von Eichborn, J.; Dunkel, M.; Macha, K.; Eckert, A.; Gilson, M. K.; Bourne, P. E.; Preissner, R. SuperTarget goes quantitative: update on drug–target interactions. *Nucleic Acids Res.* **2012**, *40*, D1113–1117.

(10) Kola, I.; Landis, J. Can the pharmaceutical industry reduce attrition rates? *Nature Rev. Drug Discovery* **2004**, *3*, 711−715.
(11) Bantscheff, M.; Eberhard, D.; Abraham, Y.; Bastuck, S.; Boesche, M.; Hobson, S.; Mathieson, T.; Perrin, J.; Raida, M.; Rau, C.; Reader, V.; Sweetman, G.; Bauer, A.; Bouwmeester, T.; Hopf, C.; Kruse, U.; Neubauer, G.; Ramsden, N.; Rick, J.; Kuster, B.; Drewes, G. Quantitative chemical proteomics reveals mechanisms of action of clinical ABL kinase inhibitors. *Nature Biotechnol.* **2007**, *25*, 1035−1044.
(12) Fischer, J. J.; Dalhoff, C.; Schrey, A. K.; Graebner, Nee; Baessler, O. Y.; Michaelis, S.; Andrich, K.; Glinski, M.; Kroll, F.; Sefkow, M.; Dreger, M.; Koester, H. Dasatinib, imatinib and staurosporine capture compounds—complementary tools for the profiling of kinases by capture compound mass spectrometry (CCMS). *J. Proteomics* **2011**, *75*, 160−168.
(13) Fischer, J. J.; Michaelis, S.; Schrey, A. K.; Diehl, A.; Graebner, O. Y.; Ungewiss, J.; Horzowski, S.; Glinski, M.; Kroll, F.; Dreger, M.; Koester, H. SAHA Capture Compound—a Novel Tool for the Profiling of Histone Deacetylases and the Identification of Additional Vorinostat Binders. *Proteomics* **2011**, *11*, 4096−4104.
(14) Bantscheff, M.; Hopf, C.; Savitski, M. M.; Dittmann, A.; Grandi, P.; Michon, A. M.; Schlegl, J.; Abraham, Y.; Becher, I.; Bergamini, G.; Boesche, M.; Delling, M.; Dumpelfeld, B.; Eberhard, D.; Huthmacher, C.; Mathieson, T.; Poeckel, D.; Reader, V.; Strunk, K.; Sweetman, G.; Kruse, U.; Neubauer, G.; Ramsden, N. G.; Drewes, G. Chemoproteomics profiling of HDAC inhibitors reveals selective targeting of HDAC complexes. *Nature Biotechnol.* **2011**, *29*, 255−265.
(15) Ieko, M. Dabigatran etexilate, a thrombin inhibitor for the prevention of venous thromboembolism and stroke. *Curr. Opin. Invest. Drugs* **2007**, *8*, 758−768.
(16) Guay, D. R. Dabigatran etexilate: a possible replacement for heparinoids and vitamin K antagonists? *Hosp. Pract.* **2011**, *39*, 105−125.
(17) Rix, U.; Hantschel, O.; Durnberger, G.; Remsing Rix, L. L.; Planyavsky, M.; Fernbach, N. V.; Kaupe, I.; Bennett, K. L.; Valent, P.; Colinge, J.; Kocher, T.; Superti-Furga, G. Chemical proteomic profiles of the BCR-ABL inhibitors imatinib, nilotinib, and dasatinib reveal novel kinase and nonkinase targets. *Blood* **2007**, *110*, 4055−4063.
(18) Fischer, J. J.; Michaelis, S.; Schrey, A. K.; Graebner, O. G.; Glinski, M.; Dreger, M.; Kroll, F.; Koester, H. Capture compound mass spectrometry sheds light on the molecular mechanisms of liver toxicity of two Parkinson drugs. *Toxicol. Sci.* **2010**, *113*, 243−253.
(19) Dalhoff, C.; Huben, M.; Lenz, T.; Poot, P.; Nordhoff, E.; Koster, H.; Weinhold, E. Synthesis of *S*-adenosyl-L-homocysteine capture compounds for selective photoinduced isolation of methyltransferases. *ChemBioChem* **2010**, *11*, 256−265.
(20) Hauel, N. H.; Nar, H.; Priepke, H.; Ries, U.; Stassen, J. M.; Wienen, W. Structure-based design of novel potent nonpeptide thrombin inhibitors. *J. Med. Chem.* **2002**, *45*, 1757−1766.
(21) Dullweber, F.; Stubbs, M. T.; Musil, D.; Sturzebecher, J.; Klebe, G. Factorising ligand affinity: a combined thermodynamic and crystallographic study of trypsin and thrombin inhibition. *J. Mol. Biol.* **2001**, *313*, 593−614.
(22) Fischer, J. J.; Graebner Baessler, O. Y.; Dalhoff, C.; Michaelis, S.; Schrey, A. K.; Ungewiss, J.; Andrich, K.; Jeske, D.; Kroll, F.; Glinski, M.; Sefkow, M.; Dreger, M.; Koester, H. Comprehensive Identification of Staurosporine-Binding Kinases in the Hepatocyte Cell Line HepG2 Using Capture Compound Mass Spectrometry (CCMS). *J. Proteome Res.* **2010**, *9*, 806−817.
(23) Sun, B.; Hoshino, J.; Jermihov, K.; Marler, L.; Pezzuto, J. M.; Mesecar, A. D.; Cushman, M. Design, synthesis, and biological evaluation of resveratrol analogues as aromatase and quinone reductase 2 inhibitors for chemoprevention of cancer. *Bioorg. Med. Chem.* **2010**, *18*, 5352−5366.
(24) Hsieh, T. C.; Wu, J. M. Resveratrol: biological and pharmaceutical properties as anticancer molecule. *Biofactors* **2010**, *36*, 360−369.
(25) Hsieh, T. C.; Wang, Z.; Hamby, C. V.; Wu, J. M. Inhibition of melanoma cell proliferation by resveratrol is correlated with upregulation of quinone reductase 2 and p53. *Biochem. Biophys. Res. Commun.* **2005**, *334*, 223−230.
(26) Rix, U.; Hantschel, O.; Durnberger, G.; Remsing Rix, L. L.; Planyavsky, M.; Fernbach, N. V.; Kaupe, I.; Bennett, K. L.; Valent, P.; Colinge, J.; Kocher, T.; Superti-Furga, G. Chemical proteomic profiles of the BCR-ABL inhibitors imatinib, nilotinib, and dasatinib reveal novel kinase and nonkinase targets. *Blood* **2007**, *110*, 4055−63.
(27) Dunstan, M. S.; Barnes, J.; Humphries, M.; Whitehead, R. C.; Bryce, R. A.; Leys, D.; Stratford, I. J.; Nolan, K. A. Novel inhibitors of NRH:quinone oxidoreductase 2 (NQO2): crystal structures, biochemical activity, and intracellular effects of imidazoacridin-6-ones. *J. Med. Chem.* **2011**, *54*, 6597−6611.
(28) Yan, C.; Dufour, M.; Siegel, D.; Reigan, P.; Gomez, J.; Shieh, B.; Moody, C. J.; Ross, D. Indolequinone Inhibitors of NRH:Quinone Oxidoreductase 2. Characterization of the Mechanism of Inhibition in both Cell-Free and Cellular Systems. *Biochemistry* **2011**, *50*, 6678−6688.
(29) Wienen, W.; Stassen, J. M.; Priepke, H.; Ries, U. J.; Hauel, N. In vitro profile and ex vivo anticoagulant activity of the direct thrombin inhibitor dabigatran and its orally active prodrug, dabigatran etexilate. *Thromb. Haemostasis* **2007**, *98*, 155−162.
(30) Kuntz, I. D.; Chen, K.; Sharp, K. A.; Kollman, P. A. The maximal affinity of ligands. *Proc. Natl. Acad. Sci. U.S.A* **1999**, *96*, 9997−10002.
(31) Reynolds, C. H.; Tounge, B. A.; Bembenek, S. D. Ligand binding efficiency: trends, physical basis, and implications. *J. Med. Chem.* **2008**, *51*, 2432−2438.
(32) Buryanovskyy, L.; Fu, Y.; Boyd, M.; Ma, Y.; Hsieh, T. C.; Wu, J. M.; Zhang, Z. Crystal structure of quinone reductase 2 in complex with resveratrol. *Biochemistry* **2004**, *43*, 11417−11426.
(33) Shen, J.; Barrios, R. J.; Jaiswal, A. K. Inactivation of the quinone oxidoreductases NQO1 and NQO2 strongly elevates the incidence and multiplicity of chemically induced skin tumors. *Cancer Res.* **2010**, *70*, 1006−1014.
(34) Long, D. J., 2nd; Iskander, K.; Gaikwad, A.; Arin, M.; Roop, D. R.; Knox, R.; Barrios, R.; Jaiswal, A. K. Disruption of dihydronicotinamide riboside:quinone oxidoreductase 2 (NQO2) leads to myeloid hyperplasia of bone marrow and decreased sensitivity to menadione toxicity. *J. Biol. Chem.* **2002**, *277*, 46131−46139.
(35) Vella, F.; Ferry, G.; Delagrange, P.; Boutin, J. A. NRH:quinone reductase 2: an enzyme of surprises and mysteries. *Biochem. Pharmacol.* **2005**, *71*, 1−12.
(36) Luo, Y.; Blex, C.; Baessler, O.; Glinski, M.; Dreger, M.; Sefkow, M.; Koster, H. The cAMP capture compound mass spectrometry as a novel tool for targeting cAMP-binding proteins: from protein kinase A to potassium/sodium hyperpolarization-activated cyclic nucleotide-gated channels. *Mol. Cell. Proteomics* **2009**, *8*, 2843−2845.
(37) Bradford, M. M. A rapid and sensitive method for the quantitation of microgram quantities of protein utilizing the principle of protein−dye binding. *Anal. Biochem.* **1976**, *72*, 248−254.
(38) Morita, T.; Jackson, C. M. Preparation and properties of derivatives of bovine factor X and factor Xa from which the gamma-carboxyglutamic acid containing domain has been removed. *J. Biol. Chem.* **1986**, *261*, 4015−4023.
(39) Jain, A. N. Morphological similarity: a 3D molecular similarity method correlated with protein−ligand recognition. *J. Comput.-Aided Mol. Des.* **2000**, *14*, 199−213.